



# The optimization of ship weather-routing algorithm based on the composite influence of multi-dynamic elements

Yu-Hsien Lin<sup>a,b</sup>, Ming-Chung Fang<sup>a,\*</sup>, Ronald W. Yeung<sup>c</sup>

<sup>a</sup>Department of Systems & Naval Mechatronic Engineering, National Cheng-Kung University, Tainan City 70101, Taiwan

<sup>b</sup>International Wave Dynamics Research Center, National Cheng-Kung University, Tainan City 70101, Taiwan

<sup>c</sup>Department of Mechanical Engineering, University of California at Berkeley, Berkeley, CA 94720-1740, USA

## ARTICLE INFO

### Article history:

Received 19 October 2012

Received in revised form 30 July 2013

Accepted 30 July 2013

### Keywords:

Ship routing

WW3

Added resistance

Speed loss

3DMI

## ABSTRACT

This study proposes a ship weather-routing algorithm based on the composite influence of multi-dynamic elements for determining the optimized ship routes. The three-dimensional modified isochrone (3DMI) method utilizing the recursive forward technique and floating grid system for the ship tracks is adopted. The great circle sailing (GCR) is considered as the reference route in the earth coordinate system. Illustrative optimized ship routes on the North Pacific Ocean have been determined and presented based on the realistic constraints, such as the presence of land boundaries, non-navigable sea, seaway influences, roll response as well as ship speed loss. The proposed calculation method is effective for optimizing results by adjusting the weighting factors in the objective functions. The merits of the proposed method can be summarized as: (1) the navigability of the route can be analyzed dynamically to acquire the optimal route; (2) adopting multi-dynamic elements as weighting factors has the benefits in energy efficiency, time-saving and minimum voyage distance; and (3) an ability to enhance speed performance and to incorporate safety concern in a dynamic environment.

© 2013 Elsevier Ltd. All rights reserved.

## 1. Introduction

It is well known that ship weather-routing is defined as a procedure to determine an optimal route based on the weather forecasts, the characteristics of a specific ship, and sea states for a particular voyage [1–3]. The optimal route can be regarded as the voyage route with safety and comfort [4,5], maximum energy efficiency [2,6,7], minimum time consumption [8,9], or the combinations of these factors [1,10] under the encountering weather circumstances. The reliability of the optimal route derived from the ship weather routing system is based on the following parameters: (i) the accuracy of the estimation of ship hydrodynamics; (ii) the quality of weather forecasting data; and (iii) the applicability of ship routing optimization.

In this paper, the optimization of ship routing algorithm along with the precise weather forecasting data and ship characteristics has been developed and evaluated. There have been some popular routing algorithms for minimizing fuel consumption or passage time, e.g. the calculus of variations [11], the modified isochrone method [12,13], the isopone method [14,15], the two-dimensional dynamic programming [6,16] and the three-dimensional dynamic programming [3]. In addition to above-mentioned algorithms, many other approaches have also been applied to solve these problems, such as the iterative dynamic programming [17], the augmented Lagrange multiplier [18],

the Dijkstra algorithm [1,19] and the genetic algorithm [20].

An access to obtaining the optimal ship route has attracted attention of researchers, Navy and shipping organizations due to its safety and efficiency concern [21]. In order to make the routing decision better, a recursive forward algorithm with floating grid system of three-dimensional modified isochrones (3DMI hereinafter) method is suggested here and evaluated in the eastbound voyages of North Pacific Ocean. The input data derived from the weather forecasts and ship hydrodynamics can be utilized to determine the criteria and optimal routes in the network graph. The advantage of present method is to achieve the expected time arrival (ETA) with the minimum fuel consumption and the minimum passage time based on the constraints of safety and land avoidance.

## 2. Ship hydrodynamics

Seakeeping characteristics of a ship includes six degrees of freedom (DOF) motions in waves and the illustrations of motions are indicated as in Fig. 1.

In the study, the fluid is assumed to be ideal, incompressible, inviscid and irrotational, and the ship travels with constant speed  $V$  in regular waves. Based on the linearity assumption, the incident wave amplitude and ship motion are assumed to be small. The relationship between the body-fixed coordinate system,  $o$ -xyz, and the inertial coordinate system,  $O$ -XYZ, is shown in Fig. 2 and given by

$$X = x + Vt; \quad Y = y; \quad Z = z \quad (1)$$

\* Corresponding author. Tel.: +886 6 2747018x211; fax: +886 6 2080592.

E-mail address: [fangmc@mail.ncku.edu.tw](mailto:fangmc@mail.ncku.edu.tw) (M.-C. Fang).

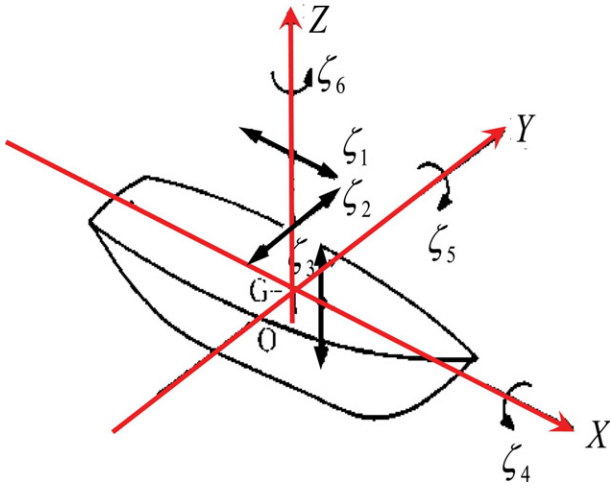


**Fig. 1.** The schematic diagram of 6 DOF motions for a ship advancing in waves. ( $\xi_1$ : surge displacement;  $\xi_2$ : sway displacement;  $\xi_3$ : heave displacement;  $\xi_4$ : roll angle;  $\xi_5$ : pitch angle;  $\xi_6$ : yaw angle).

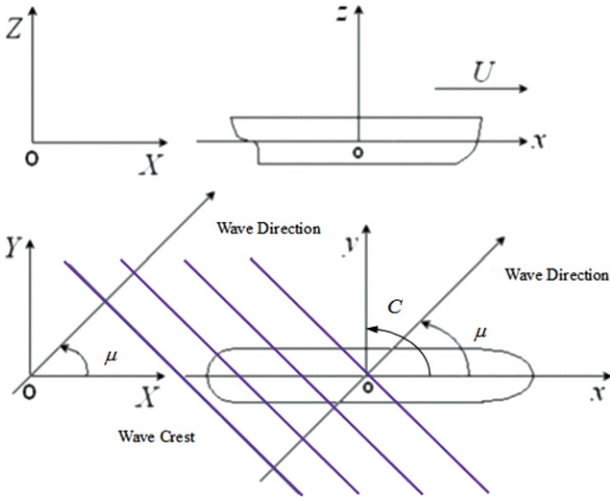


**Fig. 2.** The illustration of the ship's track in the earth-fixed coordinate system O-XYZ. (C: ship course angle calculated by the great circle algorithm;  $\mu$ : wave heading angle).

By combining the wave exciting force  $F_j^{(e)}$ , generalized added mass  $A_{jk}$ , generalized damping coefficient  $B_{jk}$  and the hydrostatic restoring force  $C_{jk}$ , the equation of motion can be formulated as

$$\sum_{k=1}^6 \left[ -\omega_e^2 (M + A_{jk}) - i\omega B_{jk} + C_{jk} \right] \zeta_k = F_j^{(e)}, \quad (2)$$

$j, k = 1, 2, \dots, 6$

where the subscript  $j, k = 1, 2, \dots, 6$  represent surge, sway, heave, roll, pitch and yaw, respectively. The symbol  $i$  is used as the imaginary number in Eq. (2).  $M$  is the mass or mass of moment inertia of the ship,  $\omega_e$  the encounter frequency, and  $\zeta_k$  the motion displacement. It is noted that the wave exciting force  $F_j^{(e)}$  and motion displacement  $\zeta_k$  are represented by the complex numbers.

Since one of the key concepts in seakeeping analysis is wave spectra, it is often useful to define idealized wave spectra which generally represent the characteristics of real wave spectra. In order to find the significant values of ship response, the following ISSC spectrum for the short-crested waves is adopted.

$$S(\omega, \mu) = \frac{172.75 H_s^2}{T^4 \omega^5} \exp\left(\frac{-691}{T^4 \omega^4}\right) \cdot \frac{2}{\pi} \cos^2 \mu \quad (3)$$

where  $H_s$ : the significant wave height;  $T$ : the mean wave period;  $\omega$ : the wave frequency.

Generally, the various responses of the vessel in irregular waves are represented by corresponding transfer functions, termed as RAO (response amplitude operator). Assume  $|\zeta_k|/a$  represents the general definition for calculated RAO of ship response; then the corresponding significant value, i.e.  $(|\zeta_k|)_{1/3}$  can be obtained by

$$(|\zeta_k|)_{1/3} = 2 \sqrt{\int_0^\infty \int_{-\pi/2}^{\pi/2} \left(\frac{|\zeta_k|}{a}\right)^2 S(\omega, \mu) d\mu d\omega}, \quad j = 1, 2, \dots, 6 \quad (4)$$

$(|\zeta_k|)_{1/3}$ : the significant values of the motion displacements;  $a$ : the incident wave amplitude.

It is noted that the significant values of RAOs,  $(|\zeta_k|)_{1/3}$ , would be calculated at any encountered sea state with respect to the significant wave height, the mean wave period, the primary wave direction and the mean ship speed, which serves as a database in advance for further evaluation of the present 3DMI method. In addition,  $(|\zeta_k|)/a$  on the right hand side of Eq. (4) is the function of  $\omega, \mu$  and  $V$ .

The added resistance and the drifting force are the resultant second-order nonlinear forces when the ship sails in waves. Since the added resistance results in the additional horse power required to keep the desired ship speed, it significantly affects the ship performance in rough seas. The calculation of the added resistance in the present paper uses the technique similar to the previous work [22] based on the weak scatter assumption [23], i.e.  $\phi_B \ll \phi_I$ , which assumes that the quadratic term and the steady potential term  $\phi_B$  are small compared with the incident wave potential  $\phi_I$ . With the solution of the corresponding potentials and motion response, the mean second-order steady-state hydrodynamic force suggested by previous literatures [24–27] is addressed in the following formula.

$$\bar{F} = \text{Re} \left\{ -\frac{1}{2} \rho \iint_{S_B} \left[ \phi_B \frac{\partial}{\partial n} - \frac{\partial \phi_B}{\partial n} \right] \nabla \phi_I^* \cdot dS \right\} \quad (5)$$

where  $\phi_I^*$  is the conjugate of the incident wave potential  $\phi_I$  and  $\phi_B$  is the disturbance potential caused by the oscillatory ship motions that can be described as the sum of the diffraction potential  $\phi_D$  and the radiation potential  $\phi_{Rj}$ .

$$\phi_B = \sum_{k=1}^6 \zeta_k \phi_{Rk} + \phi_D \quad (6)$$

The mean longitudinal force, viz. added resistance  $\bar{F}_D$ , on the ship with respect to wave heading angle in short crested waves can be written as

$$\bar{F}_D = 2 \int_0^\infty \int_{-\pi/2}^{\pi/2} \frac{F_D(\omega, \mu)}{a^2} S(\omega, \mu) d\omega d\mu \quad (7)$$

where  $F_D(\omega, \mu)$  is the added resistance component with respect to different wave heading and frequency.

Since the added resistance is also the essential characteristics for a ship in the prevailing wave conditions, a set of added resistance over a range of ship speeds with respect to different sea states can be pre-computed and served as the database for the decision of the ship optimal routing. The encountered responses of the ship at a given sea state, including added resistance, wave loads and motions, can then be determined fairly simply by interpolating the assigned values from the developed database, i.e. determining the relevant quantities needed in the route optimization.

### 3. Objective function of routing optimization

Generally, the influential parameters of ship routing optimization can be related to two aspects: involuntary and voluntary speed reduction. Involuntary speed reduction occurs because of the increased resistance in a seaway whereas the voluntary ship speed is chosen by



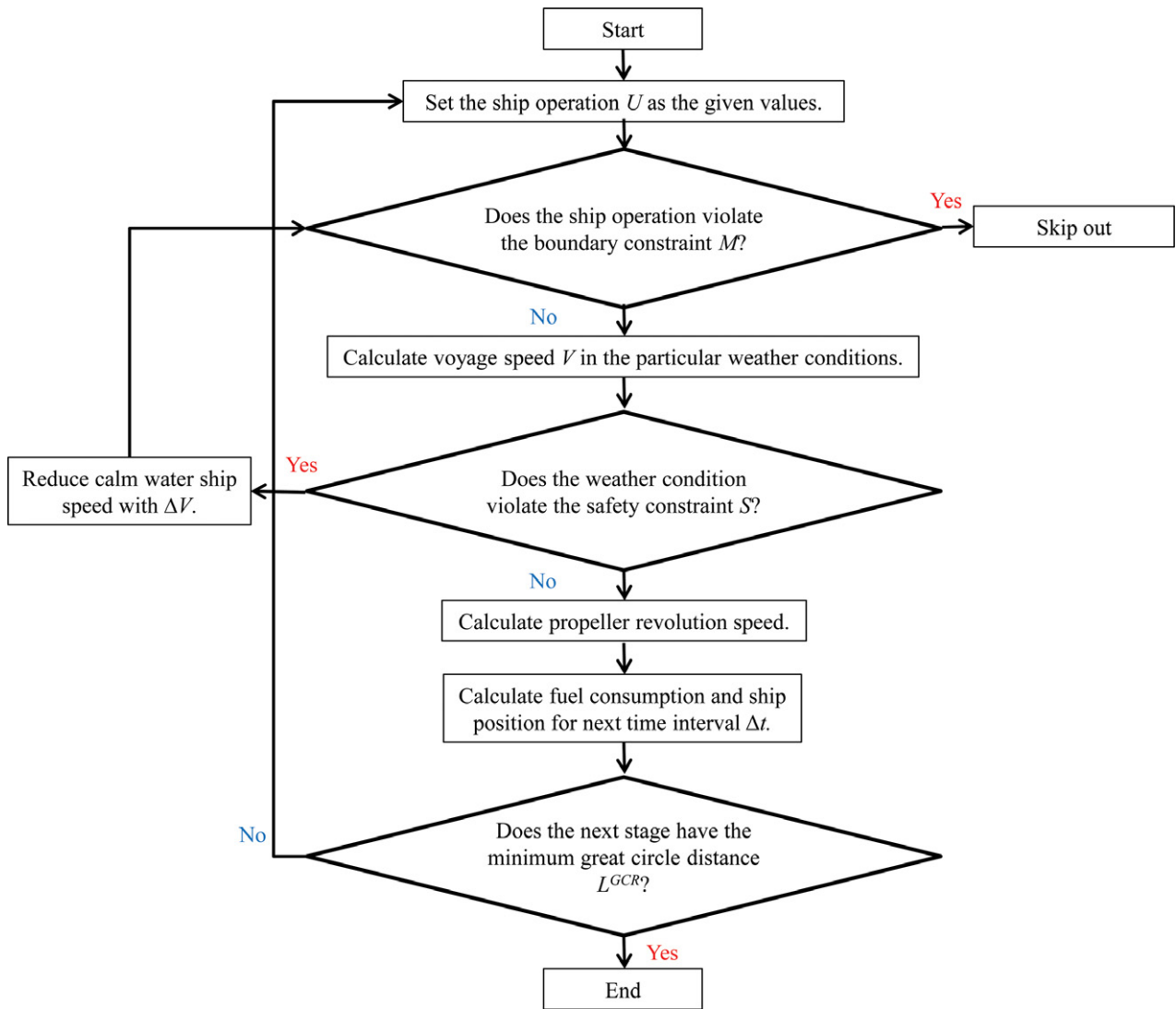


Fig. 5. The flow chart showing the procedure for determining the optimal route of a given ship operation between two stages.

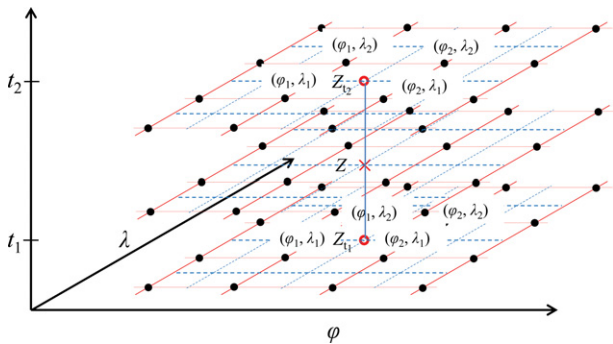


Fig. 6. The interpolation for the spatial and temporal grids.

should be modified stage by stage. The term “stage” means each segment of a voyage route between two isochrones (time fronts) after ship operation is made based on the calm-water speed assumption. Each stage is composed of several states, which are the potential geographical locations associated with ship motion responses under certain weather/sea conditions. Some of the measurable conditions of a specific ship can be shown as control variables of stage: voyage progress, fuel consumption or passage time. If the voyage progress or

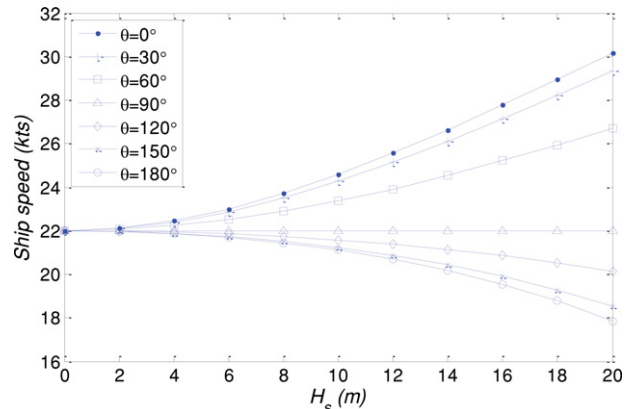


Fig. 7. The effect of wave added resistance on the ship speed with respect to different wave heading angles at propeller rpm 91 and effective power 33,760 PS.

fuel consumption is taken as the control variables of stage, passage time would be defined as the state of stage and vice versa. This study utilizes the voyage speed as the control variables of stage due to the consideration of reduced speed during a fixed passage time. Once the

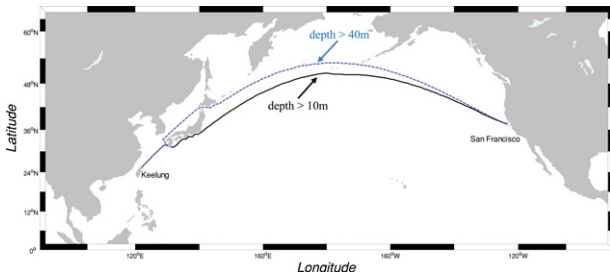


Fig. 8. The comparison of navigability for the transoceanic voyages over the water depth between 10 m and 40 m, respectively.

initial voyage course is predefined after graphical search for avoiding sea mine, the ship speed and passage time can be flexible according to the route plan, in which the power for maintaining the engine revolution speed is set constant between two neighboring stages.

### 3.1. 3DMI method

The 3DMI method in this study employs the floating grid system to define the spatiotemporal layouts for ship routing optimization. Since the instantaneous water depth and weather conditions change with time, which would modify the planned routes in the voyage correspondingly. Consequently, the navigability of a planned route based on the constraints should be analyzed dynamically according to the ocean environments. On the other hand, whether the ship speed in calm water exceeds the critical speed should also be considered as the constraints. Thus, a series of voyage progresses should be flexible according to the specific ship operations with respect to dynamic ocean environments.

Since the great circle route is the shortest distance from the departure to the destination points, it is chosen as the reference voyage route when constructing the floating grid system in the ship routing optimization. In the floating grid system, the states of each stage are three-dimensional, viz. geographical locations, passage time and the unit spacing of the course angle from the great circle route. The farthest states of a stage from the initial course are the locations which the ship based on the speed in calm water may reach within the limited passage time to avoid the harsh weather or obstacles. Voyage progresses would be deleted once the obstacles exist in the passage. It is worth to point out that the voyage speed as the control variable of a stage in the 3DMI is floating according to the voluntary and involuntary ship speeds. It is calculated based on the recursive procedure of forward algorithm.

Fig. 3 shows an example of state projections on a geophysical coordinate system from the departure to the destination points along the voyage route. The ship course followed is calculated from the great circle route which can be defined by  $C = C_0 \pm i\Delta C$ , where  $i = 0, 1, 2, \dots, N$ ; then the initial course  $C_0$  is updated as  $C$  while the ship's performance is recorded at each change. That is, the voyage progress can be deduced and recorded at each state as the course change is made. The states can be referenced by  $X_{i,j,k}$ , and the set of states at time  $t_{i,j,k}$  defines the first isochrone. The states at the first isochrone are now chosen to be the new departure point, whereby  $C_0$  is now updated to be the new course  $C$  of a great circle. Correspondingly, the second isochrone is defined at  $t_{i,j,k+1}$ . Then the same method is applied for subsequent isochrones prior to the arrival point. In order to save enormous computation time at each isochrone, the state with the minimum corresponding distance of great circle route would be considered as the new departure point primarily once the calm water sailing is assumed during the voyage.

However, it is necessary to incorporate the operation and environment constraints in the grid system for the present 3DMI method.

The optimum routing for minimum time or fuel consumption is formulated by continually iterating the overall voyage progresses as a function of ship operations and environmental constraints. A state  $X_{i,j,k}$  has a floating status during the iteration until the point corresponding to optimal route is obtained. Meanwhile, the advantage of using non-fixed time in the floating grid system is no need for interpolation.

In order to perform ship routing optimization by 3DMI method, it is more straightforward to treat the problem as a multi-stage decision process by discretizing the ship speed  $V$ . In this regard, ship routing is formulated as a discrete optimization problem. Thus, the sailing ship speed between two stages can be discretized as follows:

$$V_{i',j,k+1} = V_{i,k} + j\Delta V \quad (8)$$

where the superscript ' of  $i$  is used as the interim parameter at stage  $k + 1$  when performing iteration.  $V_{i',k+1}$  is the actual ship speed when the ship departs from stage  $k$  to  $k + 1$  by adopting calm water speed  $V_{i,k}$ . More evaluation details can be referred to Fig. 4.

Representing the ship's position at time  $t_{i,j,k}$  and the operation from  $t_{i,j,k}$  to  $t_{i,j,k+1}$  as a function of  $X_{i,j,k}$  and  $U_{i,j,k}$  respectively, and implementing great circle sailing to navigate a ship for  $\Delta t$  hours from the position  $X_{i,j,k}$  with the operation parameter  $U_{i,j,k}$ , the ship's position at  $t_{i,j,k+1}$  can be written as:

$$X_{i,j,k+1} = f(X_{i,j,k}, U_{i,j,k}, S_{i,j,k+1}, M_{i,j,k+1}, t_{i,j,k+1}) \quad (9)$$

where  $X = f_1(\lambda, \phi)$ : ship's position is a function of longitude  $\lambda$  and latitude  $\phi$ .  $U = f_2(V, C)$ : ship's operation is a function of ship speed  $V$  and course  $C$ .  $S = f_3(H_s, \phi)$ : ship's safety is a function of significant wave height  $H_s$  and significant roll angle  $\phi$ .  $M$ : boundary constraints or the obstacle areas.  $i = 1, 2, 3, \dots, N$ : the notation of the state;  $N$ : total number of states.  $j = 0, 1, 2, \dots, J - 1$ : the notation of the discrete speeds;  $J$ : total number of discrete speeds between two stages.  $k = 1, 2, 3, \dots, K - 1$ : the notation of the stage.  $K$ : total number of stages.

### 3.2. Ship resistance and determination of the weights

In order to employ the 3DMI method for the ship optimization, all the possible voyage progresses to the waypoints need to be discretized by means of the grid system formed by spherical coordinates. Since the time-dependent weather information varies in the area of the open sea encompassing the voyage progresses, the optimal route would be changed according to combinations of weights in the voyage progresses. Once these weights are assigned at each voyage progress, the solution to each segment of the optimal ship route is now transformed to a state where 3DMI can be applied to find the minimum weight of these states.

The weights  $W_{i,j,k}$  joining different states  $i$  during the progress of speed loss  $j$  at the stage  $k$  depend on the parameters that need to be optimized (or minimized). In order to obtain the optimal route by using constant propeller revolution speed, the parameter is assumed to be the speed loss between two stages at the fixed time interval together with the following great circle distance. More specifically, the optimal ship routing for minimum passage time would be discussed to determine the weight function based on the involuntary speed reduction, which means the speed loss due to the added resistance with constant revolution speed of engine.

In this paper, the speed loss due to the other external forces, i.e. wind, wave or current, is assumed to be limited for the entire voyage. Consequently, it could be hypothesized that the propulsion characteristics remain the same during a range of speed reduction from the calm water speed  $V$  to the reduced speed  $V_r$ . Simply speaking, the effective power  $P_E$  is assumed constant. Therefore, the effective power  $P_E$  in the presence of waves, viz.  $P_E = F_T(V_r)V_r$ , can be represented as the following formula:

$$F_T(V_r)V_r = F_R(V)V = F_T(V)V - F_A(V)V \quad (10)$$

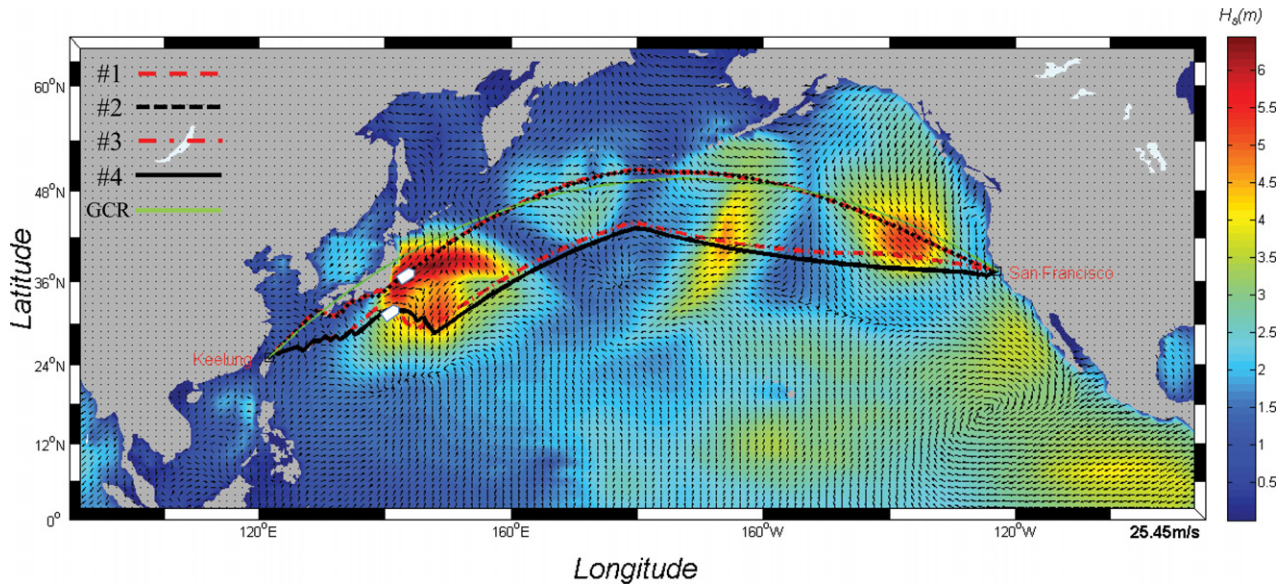


Fig. 9. The comparison of the optimal routes by considering the voyage criteria in 3DMI method. The arrow bars in the diagram indicate the wave propagating speeds and directions. The ship positions and courses for case #2 and #4 at 00:00Z on 31 May 2011 are also marked, respectively.

where  $F_T$ ,  $F_R$  and  $F_A$  are the total resistance, the still water resistance and the added resistance, respectively.

Furthermore, the reduced speed  $V_r$  can be obtained by assuming that the calm water resistance is represented in the form  $0.5\rho SC_R V^2$  and  $0.5\rho SC_R V_r^2$  [28] as the calm water speed equates  $V$  and  $V_r$ , respectively. Note that  $C_R$  is the coefficient of calm-water wave resistance. As regards the effect of added resistance, it is very important to assume that the effective power required for the reduced speed  $V_r$  is the same as the one required at speed  $V$ . Thus, Eq. (10) can be rewritten as follows:

$$0.5\rho SC_R V^2 V = 0.5\rho SC_R V_r^2 V_r + F_A(V) V \quad (11)$$

Here,  $C_R$  is considered as the constant value because we assume that the speed loss caused by added resistance is limited. In other words, the propulsion characteristics remain the same during a range of speed reduction from the calm water speed  $V$  to the reduced speed  $V_r$ .

In order to determine the reduced speed  $V_r$ , Eq. (11) can be simplified as:

$$V_r = \left( V^3 - 2 \frac{F_A(V) V}{\rho SC_R} \right)^{1/3} \quad (12)$$

The determination of added resistance in Eq. (12) is required for each state  $i$  at stage  $k$  between the neighboring nodes using the inputs of incident wave conditions and given calm-water ship speed  $V$ . The access to determining the possible state and approaching the actual arrival position is simply illustrated in Fig. 4. Specifically, once the voluntary or involuntary reduced speed for a certain voyage progress is determined, it is ready to evaluate the weights  $W_{i,j,k}$  by combining the great circle distance departing at  $k + 1$  stage  $L_{i,j,k+1}^{GCR}$ , such as:

$$w_{i,j,k} = (V_{i,j,k} - V_{i,j,k+1}) \cdot \Delta t + L_{i,j,k+1}^{GCR} \quad (13)$$

Eventually, the optimal voyage route for the shortest distance can be derived by minimizing  $W_{i,j,k}$  at each stage. However, the optimal voyage route should also include the constraints, considering the sea conditions, speed limit, land boundaries, safety and so on, for each voyage progress. More details would be discussed in the following sections.

In carrying out the shortest distance by taking into account the forecast data dynamically, the weights as indicated in Eq. (12) become an important factor to determine the optimum routing. Subsequently, the algorithm of optimal route by the 3DMI is combined with the algorithm in Eq. (13) to estimate the minimum accumulation of voyage distance. Thus, the proposed algorithm of the optimal ship route is as follows:

$$R_{opt} = \min \left\{ \sum_{k=1}^K \sum_{j=0}^{J-1} \sum_{i=1}^N w_{i,j,k} \right\} \quad (14)$$

### 3.3. Solution of voyage progress

In this study, both the voluntary and involuntary ship speeds have been executed for selecting the optimal voyage progress step-by-step. Voluntary speed loss is adopted once it is suggested to slow down the ship speed due to harsh weather conditions for ship safety. On the other hand, the involuntary speed loss due to added resistance is considered at each state for determining the actual arrival position. Since it is convenient to use ship speed in ship performance analysis, i.e. ship resistance and speed loss, the voyage speed is used as a stage control variable in this research. Subsequently, the procedure for determining the optimal route of a given ship speed between two stages is shown in Fig. 5 or can be described as follows:

1. Set the reference route by great circle algorithm and the calm water ship speed together with the initial course angle.
2. Schedule the estimated time of arrival (ETA). If the calm water ship speed is smaller than the minimum allowed ship speed of ETA or larger than the maximum allowed ship speed delivered by the engine, skip the calculation for this given course.
3. Skip out the voyage progresses violating the set constraints of safety or passing through the obstacles for a given course angle. Calculate the ship position for the next time interval by calm-water ship speed with the great circle distance between this position and the destination point.
4. Calculate the reduced ship speed by Eq. (12) and then estimate the actual arrival position recursively.

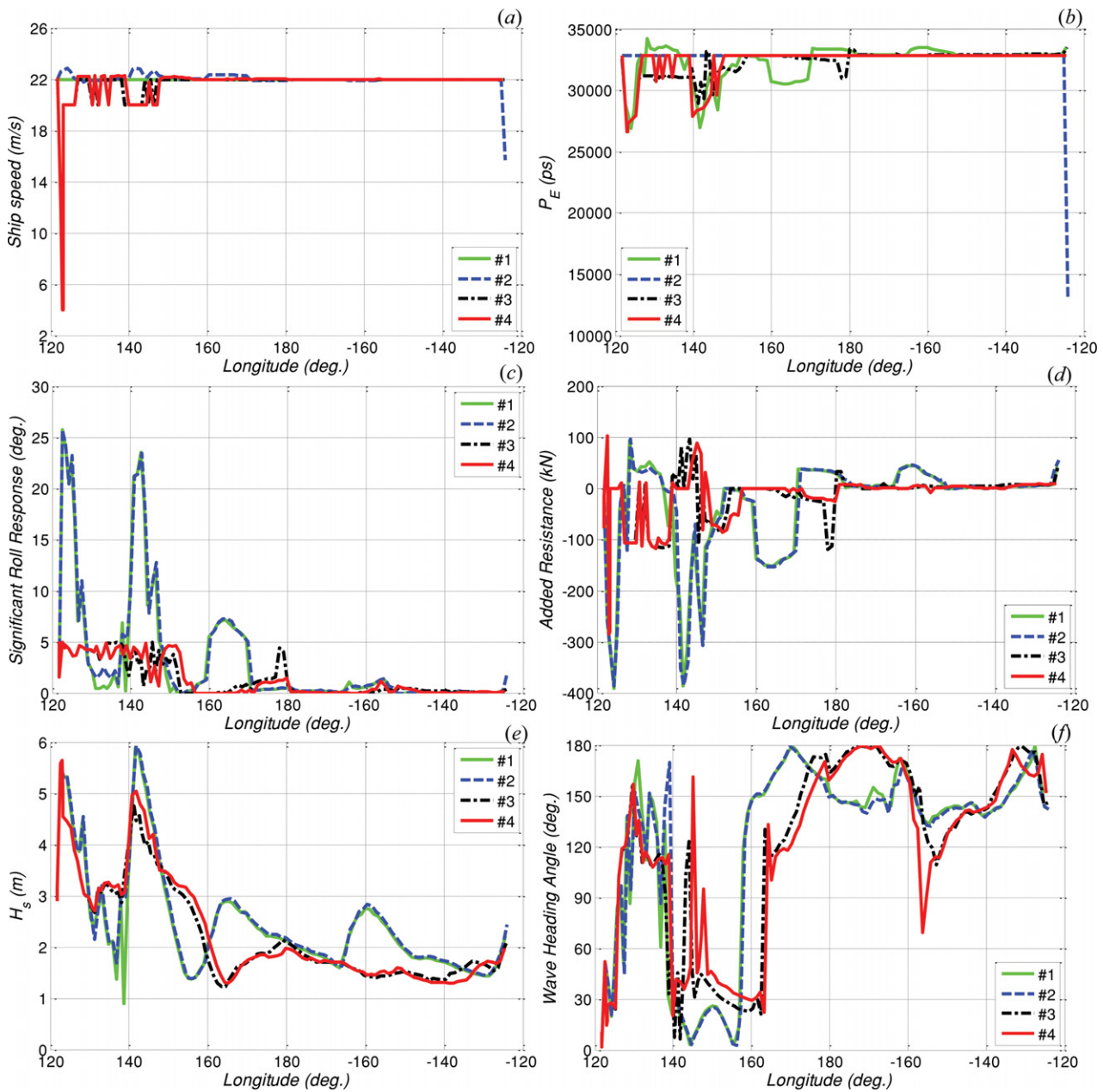


**Fig. 10.** The comparisons of ship performance for different types of route options by observing (a) ship speed; (b) effective power  $P_E$ ; (c) significant roll response; (d) added resistance; (e) significant wave height; and (f) wave heading angle.

5. Find the optimal voyage progress with the minimum great circle distance between the expected arrival point and the destination point.
6. Execute steps 1–5 repeatedly with the fixed time interval between two stages until the ship arrives at the next stage or the destination point.

#### 4. Environmental data

##### 4.2. Weather forecast data

In order to calculate the consumption needed to navigate at a desired speed and to avoid the harsh weather condition, a precise forecast of winds and waves along routes is necessary. The wave model, WAVEWATCH III (WW3 hereinafter), is the optimal solution, depending upon the desired forecast length and spatial resolution.

WW3 uses operational NCEP products as input and issues weather forecast data four times a day at 00Z, 06Z, 12Z and 18Z. The issued data set produces forecasts of every 3 h from the initial time out to 180 h. In addition, the data resolution in WW3 is  $1.25^\circ$  in longitude and  $1^\circ$  in latitude.

Since the precise ship hydrodynamics needs a rich database of WW3, the appropriate quantity and resolution of weather forecast data must be available for every leg of desired route dynamically. In the present research, both the linear and bilinear interpolation techniques are applied to interpolate the weather forecast data in the time and space dimensions, respectively. Once the ship sailing speed and the heading angle are set, the interpolated weather forecast data will search for the corresponding data sets of ship hydrodynamics. The provided forecast data of WW3 are summarized in Table 1.

**Table 1**  
The main features of the WW3 forecast data.

$\lambda$	Longitude (°)
$\varphi$	Latitude (°)
WIND	Wind speed (m/s)
WDIR	Wind dir. (°)
HTSGW	Wave height (m)
WVDIR	Wave dir. (°)
WVPER	Wave period (s)

4.2. Geographical data

The bathymetry data used for the computational domain range from  $-180.0^\circ$  E to  $180.0^\circ$  E in longitude and from  $0^\circ$  N to  $65.0^\circ$  N in latitude, with a grid resolution of  $5''$  (9260 m). The data sources were obtained from ETOPO5 data (<http://www.ngdc.noaa.gov/mgg/global/global.html>) and can be coupled with other finer grids, i.e. ETOPO1, for avoiding land collision.

4.3. Interpolation scheme for the environmental data

In the simulation of ship routing optimization, it is necessary to obtain the weather, sea and bathymetry conditions at any given time  $t$  and ship's position  $X$  using the WW3 forecast and ETOPO data sets. Thus, numerical interpolations are applied to calculate the environmental and bathymetry data in the routing algorithm. Since the numerical interpolations have to be carried out in the simulation, a simple linear interpolation scheme as shown in Fig. 6 was adopted to save computing time.

The linear interpolation over space is performed by the following equation:

$$Z = Z_{P_1} + (Z_{P_2} - Z_{P_1}) \frac{(\lambda - \lambda_1)}{(\lambda_2 - \lambda_1)} \tag{15}$$

where

$$Z_{P_1} = Z_{11} + (Z_{21} - Z_{11}) \frac{(\varphi - \varphi_1)}{(\varphi_2 - \varphi_1)}$$

$$Z_{P_2} = Z_{12} + (Z_{22} - Z_{12}) \frac{(\varphi - \varphi_1)}{(\varphi_2 - \varphi_1)}$$

$Z$ : environmental or bathymetry data at the ship's position  $(\varphi, \lambda)$ .  $Z_{11}$ ,  $Z_{12}$ ,  $Z_{21}$ ,  $Z_{22}$ : environmental or bathymetry data at the ship's position  $(\varphi_1, \lambda_1)$ ,  $(\varphi_1, \lambda_2)$ ,  $(\varphi_2, \lambda_1)$ ,  $(\varphi_2, \lambda_2)$ , surrounding the ship's position  $(\varphi, \lambda)$ .

The linear interpolation over time is conducted by the following formula:

$$Z = Z_{t_1} + (Z_{t_2} - Z_{t_1}) \frac{(t - t_1)}{(t_2 - t_1)} \tag{16}$$

where  $Z$ : environmental or bathymetry data at time  $t$ .  $Z_{t_1}$ ,  $Z_{t_2}$ : environmental or bathymetry data at time  $t_1$  and  $t_2$ .

5. Results and discussion

In this study, a container ship has been selected for the numerical simulations. The principal particulars of the hull form and performance of main engine are given in Table 2. For demonstrating the benefits of the proposed 3DMI method, numerical simulations of transoceanic voyages are conducted by considering the 3DMI method or not. Prior to the voyage simulation, the results of speed performance for varying wave heights and heading angles are exhibited for verifying the effectiveness of the present technique.

**Table 2**  
Principal particulars of the container ship.

<b>Ship</b>	
Length (m)	185.5
Breadth (m)	30.2
Depth (m)	16.6
Draft (m)	5.9
Transverse GM (m)	3.28
Vertical center of gravity (m)	12.45
Longitudinal center of gravity (m)	0.33
<b>Main engine</b>	
MCR (PS)	33,760
100% RPM	91
Service speed (kts) in calm water	22

5.1. The speed performance under different sea conditions

The speed through the water of a container ship was simulated by solving the still water resistance and added resistance in our mathematical model. Subsequently, the speeds through the water with the corresponding revolution speed 91 rpm are obtained from the open-water propeller characteristic chart provided by China Ship Building Company (CSBC, Taiwan) for various wave heights and wave headings. It should be noted that operational limits due to excessive ship's motion and accompanying dangerous phenomena are not considered in the elaboration of ship performance curves.

Fig. 7 shows the speed variation calculated by Eq. (12) under different sea conditions from the following sea ( $\theta = 0^\circ$ ) to the head sea ( $\theta = 180^\circ$ ). It is obvious that more engine power is needed in larger sea conditions than in calm water condition for maintaining a constant ship speed in the head and bow seas, whereas less engine power is required in the following and quartering stern seas. In other words, the speed performance depends greatly on the wave heading angles, especially in the strong wave areas. Thus, the ship speed is suggested to slow down for saving fuel consumption and avoiding engine damage as a ship advances in encountering bow wave conditions. On the other hand, the benefits of speed-up could be earned as a ship sails in stern wave conditions.

In this study, the fuel consumption  $C_{fuel}$  in kg per hour of the container ship is calculated by using the following formula:

$$C_{fuel} = s \cdot P_E \tag{17}$$

where  $s$  is the specific fuel consumption rate of the container ship and approximately given as  $s = 129.4$  g/BHP in accordance to ISO standard reference at MCR.

5.2. Case study: eastbound sailing of North Pacific Ocean

In order to validate the capability of the proposed 3DMI method, a series of simulations were carried out for the eastbound transoceanic voyages of a 2200 TEU container ship. On departing near Keelung City ( $25.15^\circ$  N,  $121.75^\circ$  E), Taiwan, at 0000Z on 28 May 2011, the ETA was set to 0000Z 11 June 2011 or 1500Z 11 June 2011 near San Francisco City ( $37.5^\circ$  N,  $123^\circ$  W), U.S., respectively. As mentioned in Table 3, the initial voyage speed  $V$  and passage time step  $\Delta t$  were set to the same values over two minimum navigable depths. Generally, the deeper navigable depths for transoceanic routes are highly recommended for avoiding the grounding due to the variance of tides or waves. Therefore, a set of cases by adopting water depth  $d > 40$  m (#5 – #8) would be regarded as the original voyage routes in comparison with the optimal routes by adopting water depth  $d > 10$  m (#1 – #4), which satisfies the basic requirement of safe sailing for this container ship. Meanwhile, different combinations of control parameters of 3DMI were compared in this study to obtain the optimal routes dynamically.

**Table 3**

The general descriptions of the voyage conditions. “w/” means “with”; and “w/o” represents “without”.

Case number	V (kts)	$\Delta t$ (h)	d (m)	Departure date Arrival date	Description of voyage modes
#1				2011/05/28	1. Obstacle avoidance <u>w/</u>
				00:00	2. Fixed sailing speed <u>w/</u>
				2011/06/11	3. Fixed revolution speed <u>w/o</u>
				03:00	4. Safe control mode <u>w/o</u>
#2			10	2011/05/28	1. Obstacle avoidance <u>w/</u>
				00:00	2. Fixed sailing speed <u>w/o</u>
				2011/06/11	3. Fixed revolution speed <u>w/</u>
				03:00	4. Safe control mode <u>w/o</u>
#3				2011/05/28	1. Obstacle avoidance <u>w/</u>
				00:00	2. Fixed sailing speed <u>w/</u>
				2011/06/11	3. Fixed revolution speed <u>w/o</u>
				15:00	4. Safe control mode <u>w/</u>
#4	22	3		2011/05/28	1. Obstacle avoidance <u>w/</u>
				00:00	2. Fixed sailing speed <u>w/o</u>
				2011/06/11	3. Fixed revolution speed <u>w/</u>
				15:00	4. Safe control mode <u>w/</u>
#5				2011/05/28	1. Obstacle avoidance <u>w/</u>
				00:00	2. Fixed sailing speed <u>w/</u>
				2011/06/11	3. Fixed revolution speed <u>w/o</u>
				15:00	4. Safe control mode <u>w/o</u>
#6			40	2011/05/28	1. Obstacle avoidance <u>w/</u>
				00:00	2. Fixed sailing speed <u>w/o</u>
				2011/06/11	3. Fixed revolution speed <u>w/</u>
				15:00	4. Safe control mode <u>w/o</u>
#7				2011/05/28	1. Obstacle avoidance <u>w/</u>
				00:00	2. Fixed sailing speed <u>w/</u>
				2011/06/11	3. Fixed revolution speed <u>w/o</u>
				15:00	4. Safe control mode
#8				2011/05/28	1. Obstacle avoidance <u>w/</u>
				00:00	2. Fixed sailing speed <u>w/o</u>
				2011/06/11	3. Fixed revolution speed <u>w/</u>
				15:00	4. Safe control mode <u>w/</u>

Fig. 8 displays the Mercator's projection of two shortest distance routes based on the great circle algorithm over separate navigable grids, i.e.  $d > 10$  m and  $d > 40$  m. For avoiding the sea mines across the voyage routes, it is necessary to update the collection of obstacle areas repeatedly according to given passage time and analyze the navigability of the routes. The results indicate that the calculated distance by adopting the navigable grids  $d > 10$  m is 66.7 nm shorter

than  $d > 40$  m. Subsequently, the discussions of the ship behaviors and the voyage routes by considering the individual control parameters would be conducted in the following.

When the container ship departs for San Francisco at 0000Z on 30 May 2011, a strong typhoon SONGDA generated on the east side of the Philippine Seas was invading the east coast of Japan. The passages would inevitably cross the typhoon event and lead to considerable

**Table 4**

The summary of the voyage results.

	#1/#5	#2/#6	#3/#7	#4/#8
Fuel consumption (ton)	1417.3/1484	1433/1491.7	1457.3/1458.6	1464.7/1464.7
Reduction rate (%)	4.49	3.94	0.09	0
Total mileage (nm)	7524/7817.1	7532/7798.4	7560/7603.3	7566.3/7566.3
Reduction rate (%)	3.75	3.42	0.57	0
Total passage time (h)	339/351	339/351	351/351	351/351
Reduction rate (%)	3.42	3.42	0	0
Max. roll response (°)	25.72/25.72	25.72/25.72	5.02/5.02	5.02/5.02
Reduction rate (%)	0	0	0	0

motion responses, fuel consumption or speed loss. Thus, a series of cases as shown in Table 3 were conducted by applying different types of voyage modes on different navigable grids. Fig. 9 implies that the routes #1 and #2 principally follow the initial great circle route except for avoiding the Japan Islands, whereas the routes #3 and #4 using safe control mode bias the routes and show the great adaptability to the dynamic environments. Moreover, the ship position for case #2 depict that the following waves might speed up the ship by using the constant engine revolution speed. On the other hand, the case #4 indicates that since the beam wave might have the great influence on the roll motion, the ship course is altered by using the safe control mode to reduce the potential roll response.

Furthermore, the data for the voyage corresponding to the cases shown in Fig. 9 are illustrated as a function of the ship positions in Fig. 10(a)–(f), respectively. These figures show the ship sailing speed, power performance, significant roll response, added resistance, significant wave height and the wave heading angle. In these figures, it is noticed for the fixed engine revolution speed that the ship sailing speeds in Fig. 10(a) of case #4 reduce rapidly at the initial stage followed by the smaller wave heading angles to decrease the significant roll response. In contrast, the ship sailing speed of case #2 increases slightly due to the benefits of following waves. However, the effective power in Fig. 10(b) presents that the required engine power of case #4 decreases evidently according to the voluntary speed loss, in comparison with the case #2 of fixed engine revolution speed. Fig. 10(c) demonstrates that the safe control modes utilized in case #3 and #4 can definitely search for the routes below the safety constraints. It is interesting to find that the variation of added resistance in case #4 as shown in Fig. 10(d) is briefly in phase with the power performance in Fig. 10(b) and wave heading angle in Fig. 10(f). The larger significant wave heights as shown in Fig. 10(e) would cause the larger responses of added resistance as shown in Fig. 10(d), especially in the following or head seas. For example, the maximum significant wave height of case #1 appears at (142.531°, 36.578°) in accordance with the most evident response of added resistance during the voyage.

Table 4 summarizes the results of fuel consumption, voyage mileage, total passage time and the maximum significant roll response for comparing the optimization of voyage routes from case #1 to #8. It is evident that the optimal routes calculated from case #1 to #4 have the better performances than the original routes from case #5 to #8 on saving fuel consumption, passage time and distance. However, it appears no difference in reducing the maximum significant roll response between the optimal routes and the original ones. Furthermore, the results present the considerable reduction on fuel consumption without applying the safe control mode, especially for the case #1. In addition, the simulations in terms of reducing total mileage and passage time show the similar results with the cases of reducing fuel consumption. By means of 3DMI method, it can be realized that the simulation with flexible engine revolution speed adjusts to the dynamic environments quite well, regardless of safety in navigation.

## 6. Summary and conclusions

In this paper, a proposed algorithm for ship routing optimization, 3DMI method, has been formulated as a multi-stage discrete process subjected to stochastic and dynamic condition. The seakeeping characteristics and the added resistance for evaluating the ship routing were calculated based on the 6 DOF mathematical model of ship hydrodynamics. Since the dynamic environments change with time, which would modify the planned routes in the voyage correspondingly, the proposed 3DMI method employs the floating grid system to define the spatiotemporal layouts for ship routing optimization. In addition, the recursive forward algorithm is applied by considering the weight as the stage variable as well as the constraints of ship performance. Eventually, some of the results can be concluded and listed as follows:

1. The involuntary speed loss calculated by our mathematical model has great dependence on the significant wave heights and wave heading angles.
2. The passage tracks through calm-water show a flexible navigability according to the requirement of limited water depth with regard to safety.
3. The passage tracks by comparing different combinations of voyage modes present an appreciable adaptability in dynamic environments, with regard to the speed performance and safety concern.
4. The voyage results indicate that the optimal routes by means of 3DMI method have better performances than the original ones for saving fuel consumption, voyage distances and passage time.
5. Regardless of safe control modes in ship routing optimization, the 3DMI method shows considerable reduction in fuel consumption, total mileage and passage time.
6. In addition, the safe control modes in the 3DMI method present a better performance on reducing the potential roll responses during the voyage than the other cases.

The purpose of this paper is to mainly focus on the capability and validity of the present 3DMI method, however it only considers one voyage simulation data. In order to make the present method more realistic, more voyage simulation data might be required and suggested to be done in the future work. Besides, the work would be more rigorous if the cost functions can be added to optimize the ship routing by adjusting different weights of control modes.

## Acknowledgments

This work is sponsored by National Science Council for Grant No. NSC 100-2917-1-564-064. The authors also acknowledge the partial support for this work provided by Research Center for Energy Technology and Strategy (RCETS), International Wave Dynamics Research Center (IWDRC) of National Cheng Kung University and the valuable data offering from CSBC.

## References

- [1] Padhy CP, Sen D, Bhaskaran PK. Application of wave model for weather routing of ships in the North Indian Ocean. *Natural Hazards* 2008;44:373–85.
- [2] Sen D, Padhy CP. Development of a ship weather-routing algorithm for specific application in North Indian Ocean region. In: *The international conference on marine technology*. Dhaka, Bangladesh: BUET; 2010, pp. 21–7.
- [3] Shao W, Zhou PL, Thong SK. Development of a novel forward dynamic programming method for weather routing. *Journal of Marine Science and Technology* 2012;17:239–51.
- [4] Maki A, Akimoto Y, Nagata Y, Kobayashi S, Kobayashi E, Shiotani S. A new weather-routing system that accounts for ship stability based on a real-coded genetic algorithm. *Journal of Marine Science and Technology* 2011;16:311–22.
- [5] Kosmas OT, Vlachos DS. Simulated annealing for optimal ship routing. *Computers & Operations Research* 2012;39:576–81.
- [6] Calvert S, Deakins E, Motte R. A dynamic system for fuel optimization Trans-Ocean. *Journal of Navigation* 1991;44:233–65.
- [7] Dewit C. Proposal for low-cost ocean weather routing. *Journal of Navigation* 1990;43:428–39.
- [8] Zhang LH, Zhang L, Peng RC, Li GX, Zou W. Determination of the shortest time route based on the composite influence of multidynamic elements. *Marine Geodesy* 2011;34:108–18.
- [9] Lunnon RW, Marklow AD. Optimization of time saving in navigation through an area of variable flow. *Journal of Navigation* 1992;45:384–99.
- [10] Hinnenthal J, Clauss G. Robust pareto-optimum routing of ships utilising deterministic and ensemble weather forecasts. *Ships and Offshore Structures* 2010;5:105–14.
- [11] Bijlsma SJ. On minimal-time ship routing. Delft: Delft University of Technology; 1975.
- [12] Hagiwara H, Spaans JA. Practical weather routing of sail-assisted motor vessels. *Journal of Navigation* 1987;40:96–119.
- [13] Hagiwara H. Weather routing of (sail-assisted) motor vessels. Delft: Delft University of Technology; 1989.
- [14] Spaans JA. New developments in ship weather routing. *Navigation* 1995;169:95–106.
- [15] Klompstra MB, Olsde CJ, Van Brunschot PKGM. The isopone method in optimal control. *Dynamics and Control* 1992;2:281–301.
- [16] Dewit C. Practical weather routing of sail-assisted motor vessels. *Journal of Navigation* 1988;41:134.
- [17] Avgouleas K. *Optimal ship routing*. Cambridge: Massachusetts Institute of Technology; 2008.
- [18] Tsujimoto M, Tanizawa K. Development of a weather adaptive navigation system considering ship performance in actual seas. In: *25th int conf on offshore mechanics and arctic engineering*. Hamburg, Germany. 2006, pp. 4–9.
- [19] Takashima K, Mezaoui B, Shoji R. On the fuel saving operation for coastal merchant ships using weather routing. *International Journal on Marine Navigation and Safety of Sea Transportation* 2009;3:401–6.
- [20] Bekker JF, Schmid JP. Planning the safe transit of a ship through a mapped minefield. *Journal of the Operations Research Society of South Africa* 2006;22:1–18.
- [21] Chen H. A stochastic dynamic program for minimum cost ship routing. Massachusetts Institute of Technology. Boston, U.S.A.; 1978.
- [22] Salvesen N. Second-order steady-state forces and moments on surface ships in oblique regular waves. In: *Int symp dynamics of marine vehicles and structures in waves*. University College London. 1974, pp. 212–26.
- [23] Newman JN. Second-order slowly-varying forces on vessels in irregular waves. In: *Int symp dynamics of marine vehicles and structures in waves*. University College London. 1974, pp. 182–6.
- [24] Fang MC. Roll reduction by rudder control for 2 ships during underway replenishment. *Journal of Ship Research* 1991;35:141–50.
- [25] Fang MC, Chen GR. On the nonlinear hydrodynamic forces for a ship advancing in waves. *Ocean Engineering* 2006;33:2119–34.
- [26] Fang MC, Wu YC, Hu DK, Lee ZY. The prediction of the added resistance for the trimaran ship with different side hull arrangements in waves. *Journal of Ship Research* 2009;53:227–35.
- [27] Lin Y-H, Fang M-C. Numerical simulation of ship dynamics for application in a weather routing system. In: *Proceedings of the 31st international conference on ocean, offshore and arctic engineering*. Rio de Janeiro, Brazil. 2012, p. OMAE2012–83515.
- [28] HSVA. Performance and analysis of ship powering tests. Hamburg; 2002.